

TORSIONAL VIBRATIONS OF DISCRETE-CONTINUOUS SYSTEMS WITH LOCAL NONLINEARITIES HAVING SOFT TYPE CHARACTERISTICS

AMALIA PIELORZ
MONIKA SKÓRA

Kielce University of Technology, Faculty of Management and Computer Modelling, Kielce, Poland
e-mail: apielorz@tu.kielce.pl; mskora@tu.kielce.pl

The paper deals with nonlinear vibration problems of multi-mass torsionally deformed mechanical systems. The systems consist of shafts connected by an arbitrary number of rigid bodies. In the systems, a local nonlinearity having a nonlinear characteristic of a soft type is introduced. The local nonlinearity is described by functions including irrational functions together with two other nonlinear functions. In the considerations, the wave approach is applied. Numerical analysis is focused on the investigation of the influence of the local nonlinearity on the behaviour of considered systems and on the determination of application ranges of the irrational functions. Exemplary numerical calculations are given for a three-mass system.

Key words: dynamics of mechanical systems, waves, nonlinear oscillations, discrete-continuous models

1. Introduction

The paper is aimed at the investigation of nonlinear torsional vibrations of discrete-continuous mechanical systems with a local nonlinearity having a characteristic of a soft type. This local nonlinearity is described by three functions. The first one includes irrational functions. The considered systems consist of shafts with circular cross-sections connected by means of rigid bodies. They belong to a certain class of discrete-continuous systems, namely to those where motion of elastic elements is described by means of the classical wave equation, and the local nonlinearities in such systems are justified by engineering

solutions in many machines and mechanisms (cf. Boiler and Seeger, 1987; Thomson, 1981).

Nonlinear vibrations of discrete systems are considered with various types of nonlinearities (cf. Hagedorn, 1981; Szemplińska-Stupnicka, 1990). Similarly to nonlinear discrete systems, various nonlinear functions can also be applied for the description of nonlinearities in discrete-continuous systems. We propose to use functions which contain quadric and cubic nonlinearities.

Some effects of local nonlinearities in discrete-continuous torsionally deformed systems have been already shown, e.g., in Nadolski and Pielorz (1997), Pielorz (1999), Pielorz and Skóra (2006). In Nadolski and Pielorz (1997), a single gear transmission with nonlinear loads on gear teeth is studied, in Pielorz and Skóra (2006) torsional multi-mass systems with a local nonlinearity having a hard type characteristic, while in Pielorz (1999) having a soft type characteristic are considered.

Considerations in the present paper are similar to those given in Pielorz (1999). The differences are in the assumed functions describing local nonlinearities. In Pielorz (1999) four functions are proposed for that, while here three functions, however on different assumptions. The inclusion of irrational functions in one of these functions can play a significant role in the description of local nonlinearities with a softening characteristic. They contain the second and third degree polynomials which are the most often applied in nonlinear dynamics of discrete systems.

The method proposed for the determination of solutions in arbitrary cross-sections of shafts in the system leads to equations with a retarded argument of the neutral type. The numerical analysis is performed for a three-mass system and is focused on the effect of local nonlinearity on displacements and dynamic moments.

2. Assumptions and governing equations

The discrete-continuous model of a multi-mass torsional system under considerations is shown in Fig. 1. It is assumed that the x -axis is parallel to the main axis of the system, and its origin coincides with the position of the left-hand end of the first shaft in an undisturbed state at the time instant $t = 0$. The i -th shaft, $i = 1, 2, \dots, N$, is characterised by length l_i , density ρ , shear modulus G and polar moment of inertia I_{0i} . The i -th rigid body connecting corresponding shafts is characterised by the mass moment of inertia J_i . A single local nonlinearity is located in the cross-section $x = 0$, and it can represent

mechanical properties of various elements, such as clutches and gears, having nonlinear characteristics of a soft type. This local nonlinearity is represented by means of the nonlinear moment M_{sp} . The rigid body J_1 is loaded by the external loading $M(t)$. Moreover, it is assumed that angular displacements θ_i and angular velocities $\partial\theta_i/\partial t$ of the shaft cross-sections of the i -th elastic element are equal to zero at time instant $t = 0$.

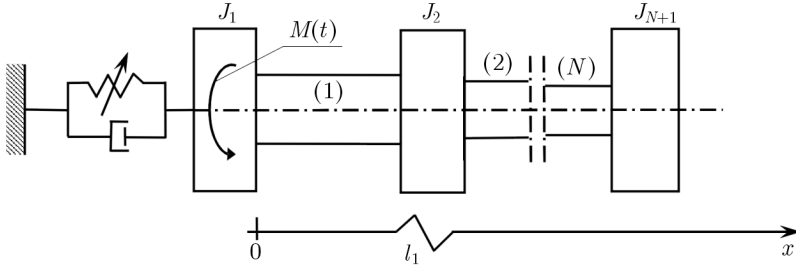


Fig. 1. Nonlinear discrete-continuous model of a torsional system

Damping in the system is described by equivalent external and internal damping taken into account in the cross-sections where rigid bodies are located. They are expressed by the following moments

$$M_{di}(t) = d_i\theta_{i,t}(x, t) \qquad M_{Di}(t) = GI_{0i}D_i\theta_{i,xt}(x, t) \qquad (2.1)$$

where d_i and D_i are coefficients of the equivalent external and internal damping, respectively, and comma denotes partial differentiation.

On the above assumptions, the determination of angular displacement $\theta_i(x, t)$ of the shaft cross-sections is reduced to solving N classical wave equations

$$\theta_{i,tt} - c^2\theta_{i,xx} = 0 \qquad i = 1, 2, \dots, N \qquad (2.2)$$

with zero initial conditions

$$\theta_i(x, 0) = \theta_{i,t}(x, 0) = 0 \qquad i = 1, 2, \dots, N \qquad (2.3)$$

and with the following nonlinear boundary conditions:

— for $x = 0$

$$M(t) - J_1\theta_{1,tt} + GI_{01}(D_1\theta_{1,xt} + \theta_{1,x}) - d_1\theta_{1,t} - M_{sp}(t) = 0 \qquad (2.4)$$

— for $x = \sum_{k=1}^i l_k, i = 1, 2, \dots, N - 1$

$$\theta_i(x, t) = \theta_{i+1}(x, t) \qquad (2.5)$$

$$-J_{i+1}\theta_{i,tt} - GI_{0i}(D_i\theta_{i,xt} + \theta_{i,x}) + GI_{0,i+1}(D_{i+1}\theta_{i+1,xt} + \theta_{i+1,x}) - d_{i+1}\theta_{i,t} = 0$$

— for $x = \sum_{k=1}^N l_k$

$$-J_{N+1}\theta_{N,tt} - GI_{0N}(D_N\theta_{N,xt} + \theta_{N,x}) - d_{N+1}\theta_{N,t} = 0 \quad (2.6)$$

where $c^2 = G/\rho$.

Upon the introduction of the following dimensionless quantities (cf. Pielorz, 1999; Pielorz and Skóra, 2006)

$$\begin{aligned} \bar{x} &= \frac{x}{l_1} & \bar{t} &= \frac{ct}{l_1} & \bar{\theta}_i &= \frac{\theta_i}{\theta_0} & \bar{d}_i &= \frac{d_i l_1}{J_1 c} \\ \bar{D}_i &= \frac{D_i c}{l_1} & \bar{l}_i &= \frac{l_i}{l_1} & B_i &= \frac{I_{0i}}{I_{01}} & K_r &= \frac{I_{01} \rho l_1}{J_1} \\ E_i &= \frac{J_1}{J_i} & \bar{M} &= \frac{M l_1^2}{J_1 c^2 \theta_0} & \bar{M}_{sp} &= \frac{M_{sp} l_1^2}{J_1 c^2 \theta_0} \end{aligned} \quad (2.7)$$

problem (2.2)-(2.6) takes the form

$$\theta_{i,tt} - \theta_{i,xx} = 0 \quad \theta_i(x, 0) = \theta_{i,t}(x, 0) = 0 \quad i = 1, 2, \dots, N \quad (2.8)$$

and

— for $x = 0$

$$M(t) - \theta_{1,tt} + K_r(D_1\theta_{1,xt} + \theta_{1,x}) - d_1\theta_{1,t} - M_{sp}(t) = 0 \quad (2.9)$$

— for $x = \sum_{k=1}^i l_k$, $i = 1, 2, \dots, N - 1$

$$\theta_i(x, t) = \theta_{i+1}(x, t) \quad (2.10)$$

$$\begin{aligned} -\theta_{i,tt} - K_r B_i E_{i+1}(D_i\theta_{i,xt} + \theta_{i,x}) + K_r B_{i+1} E_{i+1}(D_{i+1}\theta_{i+1,xt} + \theta_{i+1,x}) + \\ -E_{i+1}d_{i+1}\theta_{i,t} = 0 \end{aligned}$$

— for $x = \sum_{k=1}^N l_k$

$$-\theta_{N,tt} - K_r B_N E_{N+1}(D_N\theta_{N,xt} + \theta_{N,x}) - E_{N+1}d_{N+1}\theta_{N,t} = 0 \quad (2.11)$$

where θ_0 is a fixed angular displacement and the bars denoting dimensionless quantities are omitted for convenience.

The solutions to equations (2.8)₁ are sought in the form

$$\theta_i(x, t) = f_i(t - t_{0i} - x + x_{0i}) + g_i(t - t_{0i} + x - x_{0i}) \quad i = 1, 2, \dots, N \quad (2.12)$$

where the functions f_i and g_i represent the waves caused by external loading $M(t)$ propagating in the i -th shaft in the positive and negative senses of the

x -axis, respectively. The constants x_{0i} and t_{0i} are the cross-section and the time instant at which the first disturbance caused by the external moment $M(t)$ occurs in the i -th shaft. The functions f_i and g_i are continuous and equal to zero for negative arguments. For the system shown in Fig. 1, the constants x_{0i} and t_{0i} are equal to

$$x_{0i} = \sum_{k=1}^{i-1} l_k \qquad t_{0i} = \sum_{k=1}^{i-1} l_k \qquad (2.13)$$

Substituting solutions (2.12) with (2.13) into boundary conditions (2.9)-(2.11) and denoting the largest argument in each boundary condition separately by z , the following set of equations for the unknown functions f_i and g_i is obtained

$$\begin{aligned} r_{N+1,1}g''_N(z) + r_{N+1,2}g'_N(z) &= r_{N+1,3}f''_N(z - 2l_N) + r_{N+1,4}f'_N(z - 2l_N) \\ g_i(z) &= f_{i+1}(z - 2l_i) + g_{i+1}(z - 2l_i) - f_i(z - 2l_i) \qquad i = 1, 2, \dots, N - 1 \\ r_{11}f''_1(z) &= M(z) + r_{12}g''_1(z) + r_{13}f'_1(z) + r_{14}g'_1(z) - M_{sp}(z) \qquad (2.14) \\ r_{i1}f''_i(z) + r_{i2}f'_i(z) &= r_{i3}g''_i(z) + r_{i4}g'_i(z) + r_{i5}f''_{i-1}(z) + r_{i6}f'_{i-1}(z) \\ &\qquad i = 2, 3, \dots, N \end{aligned}$$

where

$$\begin{aligned} r_{11} &= K_r D_1 + 1 & r_{12} &= K_r D_1 - 1 \\ r_{13} &= -K_r - d_1 & r_{14} &= K_r - d_1 \\ r_{i1} &= K_r E_i (B_i D_i + B_{i-1} D_{i-1}) + 1 & r_{i2} &= E_i [K_r (B_i + B_{i-1}) + d_i] \\ r_{i3} &= K_r E_i (B_i D_i - B_{i-1} D_{i-1}) - 1 & r_{i4} &= E_i [K_r (B_i - B_{i-1}) - d_i] \\ r_{i5} &= 2K_r B_{i-1} E_i D_{i-1} & r_{i6} &= 2K_r B_{i-1} E_i \qquad i = 2, 3, \dots, N \\ r_{N+1,1} &= K_r B_N E_{N+1} D_N + 1 & r_{N+1,2} &= E_{N+1} (K_r B_N + d_{N+1}) \\ r_{N+1,3} &= K_r B_N E_{N+1} D_N - 1 & r_{N+1,4} &= E_{N+1} (K_r B_N - d_{N+1}) \end{aligned} \qquad (2.15)$$

Equations (2.14) are nonlinear differential equations with a retarded argument of the neutral type (cf. Hale, 1977; Muszyński and Myszkiś, 1984). They are the same as in Pielorz (1999). The differences lie in M_{sp} . Equations (2.14) are solved numerically by means of the Runge-Kutta method in the given sequence. The same approach is also applied in the discussion of discrete-continuous torsionally deformed systems in Szolc (2003) together with appropriate experimental confirmations.

It should be pointed out that the introduction of the common argument z in (2.14) enables us to reduce the considered problem for a multi-mass discrete-continuous torsionally deformed system to solving such a set of equations for the functions f_i and g_i which allow us to determine simultaneously all these functions from $z \geq 0$. The way used above is presented in details in Ponomarev *et al.* (1957) for a fixed rod impacted by a rigid body. Moreover, in Pielorz (1988) some comparisons are presented for special cases of the system shown in Fig. 1. That paper concerns, namely, the comparison of the approach used in the present paper with the method of the rigid finite elements, and the comparison of the results obtained for the equation of motion being a dissipative wave equation with the solution for the classical wave equation taking into account the equivalent damping in boundary conditions. In all considered cases, a good agreement of the compared results was noticed.

The function $M_{sp}(t)$ in (2.14) represents the moment for a nonlinear spring, Fig. 1. It can be described by various functions. Below, the following nondimensional functions are proposed for that

$$M_{sp}(t) = \begin{cases} k_1\theta_1(0, t) - k_w(-\theta_1(0, t))^w & \text{for } \theta_1 \leq 0 \\ k_1\theta_1(0, t) + k_w(\theta_1(0, t))^w & \text{for } \theta_1 \geq 0 \end{cases} \quad (2.16)$$

where k_1 and k_w appear at the linear and nonlinear terms, respectively, and the exponent w is assumed to be greater than 1. Nonlinear parts in (2.16) are expressed by irrational functions which give many possibilities for the description of experimental data. We are interested in the local nonlinearity having a soft type characteristic, i.e. in function (2.16) with $k_w < 0$. It should be pointed out that functions (2.16) are used in Pielorz and Skóra (2006) for the description of local nonlinearities having hard type characteristics ($k_w > 0$).

Local nonlinearities and functions of type (2.16) are justified by numerous experimental studies (cf. Boiler and Seeger, 1987). The constants k_1 and k_w are usually determined experimentally. In the case of a softening characteristic, we are interested in that part of the diagram of the function (2.16) where M_{sp} is an increasing function.

Functions (2.16) contain the second and third degree polynomials. In technical literature, in the discussion of dynamics of nonlinear discrete systems, the second and third degree polynomials are usually applied (cf. Hagedorn, 1981; Stewart *et al.*, 1995). Here, this assumption is generalised by introducing irrational functions for discrete-continuous systems.

Apart from functions (2.16) with $k_w < 0$, two following functions are proposed for the description of the nonlinear moment

$$M_{sp}(t) = A \tanh(B\theta_1) \quad (2.17)$$

or

$$M_{sp}(t) = \begin{cases} A[-1 + \exp(B\theta_1)] & \text{for } \theta_1 \leq 0 \\ A[1 - \exp(-B\theta_1)] & \text{for } \theta_1 \geq 0 \end{cases} \quad (2.18)$$

where the constants A and B are assumed to be connected with the constants w , k_1 and k_w by the relations

$$AB = k_1 \quad A = k_1\theta_m + k_w(\theta_m)^w \quad \theta_m = \left(-\frac{k_1}{wk_w}\right)^{\frac{1}{w-1}} \quad (2.19)$$

From relations (2.19), it follows that all three functions (2.16)-(2.18) describe the same linear case. Besides, functions (2.17) and (2.18) have the asymptotes $M_{sp} = \pm M_{max}$ where M_{max} are maximum values of functions (2.16) determined by w , k_w and k_1 .

3. Numerical results

The main aim of numerical calculations is the investigation of the influence of the local nonlinearity with the soft type characteristic described by functions (2.16) including irrational functions on the behaviour of the discrete-continuous systems considered.

The external moment $M(t)$ appearing in equations (2.14) can be arbitrary. Similarly to the investigations of nonlinear discrete systems, it is assumed in the form

$$M(t) = M_0 \sin(pt) \quad (3.1)$$

where p and M_0 are dimensionless frequencies and amplitudes of the external loading. The discussion is focused on the solutions in steady states.

Nonlinear effects in the considered systems are caused directly by the nonlinear moment $M_{sp}(t)$ described by functions (2.16). They are also connected with the amplitude M_0 of the external moment and with the external and internal damping. In the numerical analysis, the damping coefficients are assumed to be constant and equal to $d_i = D_i = 0.1$, k_1 is fixed and k_w , together with w , can vary.

Numerical results given below are exemplary. They are performed for the three-mass torsional system and are focused on the effect of nonlinearity on the angular displacements and on the nonlinear dynamic moment M_{sp} . All results concern solutions in the cross-section $x = 0$ where the nonlinear discrete element is introduced, though equations (2.14) allow us also to determine angular displacements in other cross-sections.

The three-mass torsional system is characterised by the following basic parameters (cf. Pielorz, 1999)

$$\begin{aligned} K_r = 0.05 & & k_1 = 0.05 & & N = 2 & & B_2 = 1 \\ l_1 = l_2 = 1 & & d_i = D_i = 0.1 & & E_2 = E_3 = 0.8 \end{aligned} \quad (3.2)$$

Diagrams of functions (2.16) with $k_w = -0.005$, $w = 1.5, 1.9, 2.25, 2.5, 3.0$ and with the linear case are presented in Fig. 2. They show how the nonlinearity becomes stronger with the increase of w .

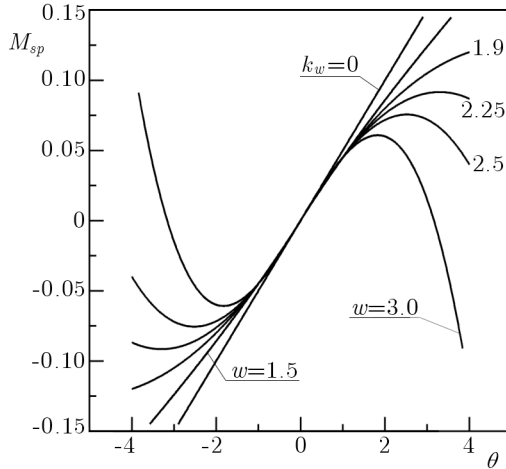


Fig. 2. Diagrams of functions (2.16)

The wave approach applied in the paper together with the Runge-Kutta method give the numerical solutions first in the transient and next in the steady states. In Fig. 3, a solution for the angular displacement versus time is presented in the cross-section $x = 0$ for $p = 0.2$, $w = 1.75$, $M_0 = 0.4$ and $k_w = -0.005$. From Fig. 3 it follows that the steady state is achieved for $t > 200$ with the displacement amplitude equal to 8.19033.

Further numerical calculations concern amplitude-frequency curves for angular displacements and for the dynamic moment. Such curves play an important role in engineering problems.

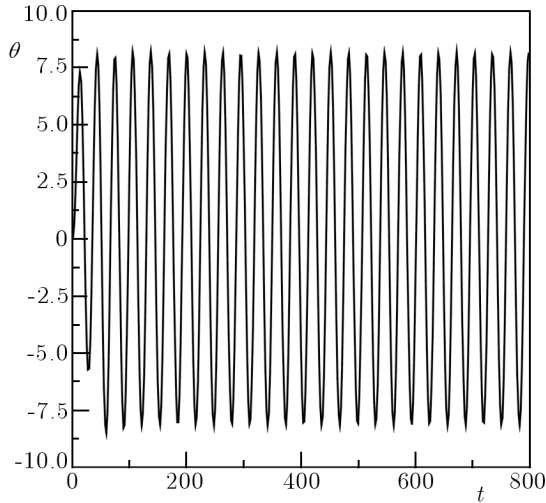


Fig. 3. Angular displacements in $x = 0$ with $p = 0.2$, $w = 1.75$, $k_w = -0.005$ and $M_0 = 0.4$

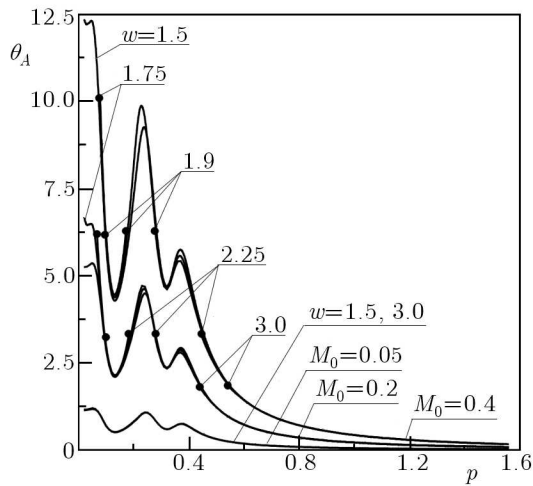


Fig. 4. Amplitude-frequency curves for angular displacements in $x = 0$ for $k_w = -0.005$, $M_0 = 0.05, 0.2, 0.4$ and with $w = 1.5, 1.75, 1.9, 2.25, 3.0$

In Fig. 4, the amplitude-frequency curves for the angular displacement in the cross-section $x = 0$ of the three-mass system are plotted with $k_3 = -0.005$, $M_0 = 0.05, 0.2, 0.4$ and for $p \leq 1.56$, using functions (2.16) for the description of the nonlinear moment M_{sp} with exponents $w = 1.5, 1.75, 1.9, 2.25, 3.0$. Nonlinear effects were observed only in the first three resonant regions ($\omega_1 = 0.089$, $\omega_2 = 0.261$, $\omega_3 = 0.376$). One would expect that the

maximal displacement amplitudes should increase with the increase of the amplitude M_0 of the external moment and with the increase of the exponent w . This is true up to the frequency p , when the solution begins to tend to infinity, i.e., when the escape phenomenon, known in nonlinear dynamics of discrete systems, occurs (cf. Stewart *et al.*, 1995). For $M_0 = 0.05$, the solutions for all exponents w are practically the same and their diagrams are identical. For higher values of the amplitude M_0 of the external moment one can notice that there exist intervals of the frequency p of the external moment where the solutions can diverge to infinity. The escape phenomenon can be observed in the first, in the first two or in the all three resonant regions, depending on w and M_0 . Namely, when $M_0 = 0.2$, function (2.16) with $w = 1.5$ and $w = 1.75$ gives always solutions behaving as a sinusoidal function with periods equal to the period of the external moment in the whole interval of p considered. The displacements are higher for $w = 1.75$. The solutions with function (2.16) are of a sinusoidal type with $w = 1.9$ for $p > 0.066$, with $w = 2.25$ for $0.095 < p < 0.183$ and $p > 0.275$, and with $w = 3.0$ for $p > 0.437$ after the third resonance. When $M_0 = 0.4$, the solutions to equations (2.14) do not diverge to infinity in the whole considered regions for functions (2.16) only with $w = 1.5$, while the escape phenomenon does not occur with $w = 1.75$ for $p > 0.077$ after the first resonant region, with $w = 1.9$ in the first two resonant regions for $0.099 < p < 0.173$ and $p > 0.277$, and with the both remaining values of the exponent w after the third resonance for $p > 0.444$ and $p > 0.544$, respectively for $w = 2.25$ and $w = 3.0$. Dots in the diagrams plotted in Fig. 4 denote the extreme values of the frequency p where the solutions cease to behave harmonically. One can notice that the angular displacements in these extreme frequencies have similar values for a fixed exponent w .

For clarity, the amplitude-frequency diagrams for the dynamic moment M_{sp} obtained by solving equations (2.14) with functions (2.16) are presented in Fig. 5 and Fig. 6, separately for $M_0 = 0.05, 0.2$ and $M_0 = 0.05, 0.4$ with the same values of exponents equal to $w = 1.5, 1.75, 1.9, 2.25, 3.0$. The diagrams in both figures include three resonant regions. For the amplitude M_0 of the external moment equal to 0.05, the linear case is obtained and the solutions for the assumed values of w coincide with each other.

When $M_0 = 0.2$ (Fig. 5), the nonlinear effects can be noticed, i.e., the escape phenomenon. The appropriate intervals of p where the solutions diverge to infinity are the same as those for angular displacements shown in Fig. 4. From Fig. 5 it follows that the escape phenomenon occurs when the dynamic moment approaches the appropriate maximum for functions (2.16) determined by the exponent w , the coefficient k_w of the nonlinear term in functions (2.16)

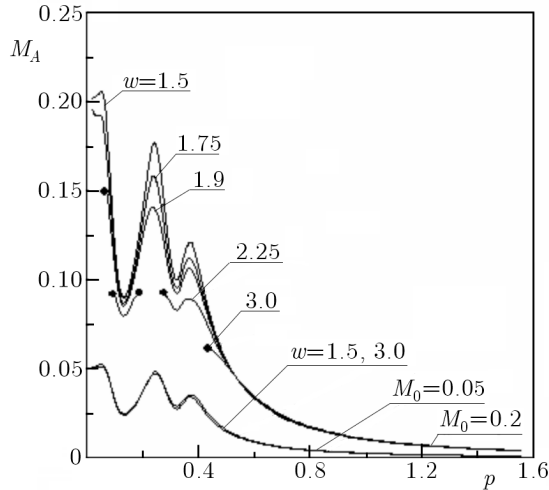


Fig. 5. Amplitudes of the dynamic moment M_{sp} for $k_w = -0.005$, $M_0 = 0.05, 0.2$ and with $w = 1.5, 1.75, 1.9, 2.25, 3.00$

and the coefficient k_1 of the linear term. For the $k_w = -0.005$, $k_1 = 0.05$, these maximum values for functions (2.16) are 0.7407, 0.2189, 0.1499, 0.0916, 0.0609 for $w = 1.5, 1.75, 1.9, 2.25$ and 3.0 , respectively. The dots in diagrams in Fig. 5 denote extreme values of the frequency p of the external moment, where the solutions cease or begin to be harmonic vibrations with periods equal to the period of the external moment. In the case of $w = 1.5$ and $w = 1.75$, the maximum of function (2.16) is never achieved, so the solutions in the whole considered region of p are harmonically changing functions in time in the steady state, and they are higher for $w = 1.5$. The appropriate maximum is achieved for all the remaining values of w : in the first resonant region for $w = 1.9$, in the first two resonant regions for $w = 2.25$, and in the three resonant regions with $w = 3.0$ for $p < 0.436$.

From the amplitude-frequency diagrams for the dynamic moment M_{sp} shown in Fig. 6 it follows that when $M_0 = 0.4$ the escape phenomenon can also be noticed. The appropriate intervals of p where the solutions diverge to infinity are the same as those for angular displacements shown in Fig. 4 with $M_0 = 0.4$. One can see that the escape phenomenon occurs when the dynamic moment approaches the appropriate maximum for functions (2.16), similarly to the results presented in Fig. 5 for $M_0 = 0.2$. The dots in diagrams in Fig. 6 denote again extreme values of the frequency p of the external moment, where the solutions cease or begin to be harmonic vibrations with periods equal to the period of the external moment. In the case of $w = 1.5$, the maximum of function (2.16) is not achieved, so the solution in the whole considered region

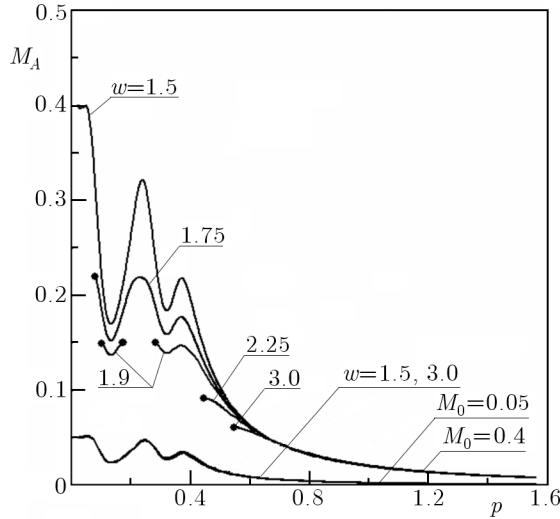


Fig. 6. Amplitudes of the dynamic moment M_{sp} for $k_w = -0.005$, $M_0 = 0.05, 0.4$ and with $w = 1.5, 1.75, 1.9, 2.25, 3.0$

of p in the steady state is a harmonic vibration. In the case of $M_0 = 0.4$, the maximum is achieved for all the remaining values of w : in the first resonant region for $w = 1.75$, in the first two resonant regions for $w = 1.9$, and in the three resonant regions for $w = 2.25$ and 3.0 in such a manner that the solutions with these exponents begin to behave as a harmonic vibration after the third resonance, namely for $p > 0.444$ and $p > 0.544$, respectively.

The diagrams in Figs 4, 5 and 6 show the effect of the exponent w on the angular displacements and on the dynamic moment. From these diagrams it also follows that the amplitude M_0 has a significant influence on the appropriate solutions of the considered nonlinear problem. It seems to be important to find amplitudes of the external moment where the solutions are harmonic vibrations, depending on the frequency p . For this reason, the application ranges of functions (2.16) are investigated for $k_w = -0.005, -0.004, -0.003$ and for $w = 1.75, 1.9, 2.25$. Suitable curves are plotted in Fig. 7. The curves for $k_w = -0.005$ are marked by solid lines, for $k_w = -0.004$ by dashed lines and for $k_w = -0.003$ by dash-dash-dot-dot lines. They determine amplitudes of the external moment below which the numerical solutions are harmonic vibrations with periods equal to the period of the external moment. The smallest values for M_0 are acceptable in the neighbourhood of the resonances. One can also see that for a fixed k_w the restrictions for the admissible values for M_0 become stronger with the increase of the exponent w . Besides, there exists an interval of p where the admissible values of M_0 increase in a linear man-

ner. This interval occurs between the first and second resonances for each w and k_w .

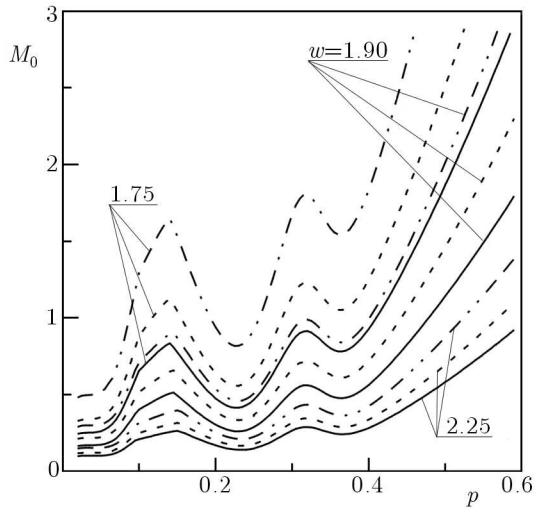


Fig. 7. Application ranges of functions (2.16) with $k_w = -0.005$ (solid lines), $k_w = -0.004$ (dashed lines), $k_w = -0.003$ (dash-dash-dot-dot lines) for $w = 1.75, 1.9, 2.25$

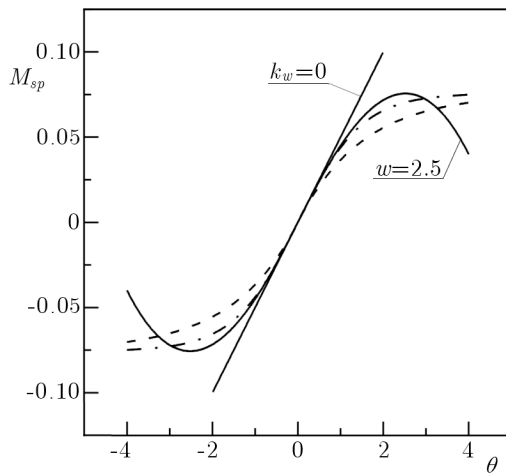


Fig. 8. Diagrams of function (2.16) (solid line), function (2.17) (- · - · -) and function (2.18) (dashed line)

The main aim of the paper is to investigate the possibility of application of the functions containing irrational functions in the description of the local nonlinearity in multi-mass torsional systems. However, from Figs 4-7 it follows

that there exist situations connected with the escape phenomenon where the use of functions (2.16) is not convenient. Then other nonlinear functions ought to be applied in the discussion of nonlinear discrete-continuous systems, including hyperbolic tangent functions (2.17) and exponential functions (2.18). Functions (2.16)-(2.18) are connected by relations (2.19), which means that they give the same linear case. Besides, functions (2.17) and (2.18) have the asymptotes $M_{sp} = \pm M_{max}$ where M_{max} are maximum values of functions (2.16). This is seen from diagrams of functions (2.16), (2.17) and (2.18) with $k_w = -0.005$, $w = 2.5$, $k_1 = 0.05$ shown in Fig. 8, together with the linear case.

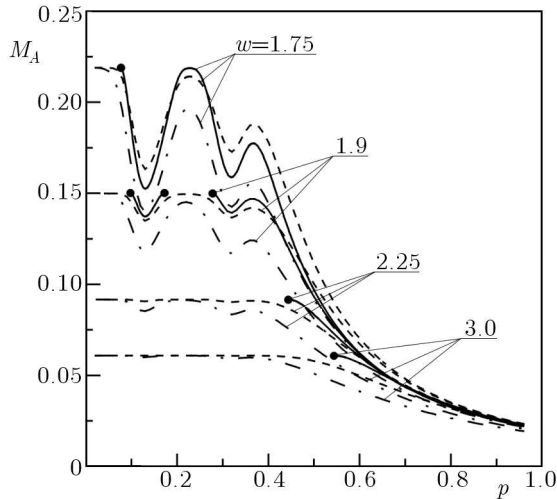


Fig. 9. Amplitudes of the dynamic moment M_{sp} for $k_w = -0.005$, $M_0 = 0.4$, $w = 1.75, 1.9, 2.25, 3.0$ using functions (2.16) (solid lines), hyperbolic tangent function (2.17) (dashed lines) and exponential function (2.18) (dash-dot lines)

A comparison of the results obtained using functions (2.16) (solid lines), hyperbolic tangent function (2.17) (dashed lines) and exponential function (2.18) (dash-dot lines) as M_{sp} is presented in Fig. 9 with $k_w = -0.005$, $M_0 = 0.4$ and for $w = 1.75, 1.9, 2.25, 3.0$. This is done for the amplitude-frequency curves of the dynamic moment for $p < 0.97$. For $p > 0.97$, the suitable diagrams coincide for all three functions describing the local nonlinearity having the characteristic of a soft type. From Fig. 9 it follows that for a fixed p , the application of hyperbolic tangent function (2.17) gives usually slightly higher values of the solution than exponential function (2.18). The differences between them become smaller for higher values of the exponent w . Moreover,

the use of function (2.17) leads to results closer to the results corresponding to function (2.16) than to exponential function (2.18). As it follows from the diagrams in Fig. 9, nonlinear functions (2.17) and (2.18) have no restrictions for their application in the description of the local nonlinearity. In the resonant regions, where the solutions with function (2.17) diverge to infinity, the solutions with functions (2.17) and (2.18) take the form of a plateau.

4. Final remarks

From the considerations in the paper, it follows that nonlinear functions containing irrational functions can be applied for the description of local nonlinearities with soft type characteristics in multi-mass discrete-continuous torsional systems using the wave approach. Appropriate studies on the nonlinear dynamics of discrete systems mainly concern quadric or cubic nonlinearities. Here, problems for nonlinear vibrations of discrete-continuous systems are formulated, and the use of irrational functions enables one to assume not only integers as exponents in local nonlinearities.

Numerical calculations concern the effect of parameters occurring in nonlinear functions containing irrational functions on the behaviour of the three-mass system. This effect is observed in the first three resonant regions. It appears that the irrational functions have some restrictions on their application which are connected with the occurrence of the escape phenomenon. The application ranges shown in Fig. 7 include cases when the escape phenomenon is observed and where other nonlinear functions ought to be used instead of functions expressed by the irrational functions. In the present paper, a hyperbolic tangent function and an exponential function are proposed for that.

Analogous calculations were also performed for nonlinear vibrations of a two-mass torsional system. Nonlinear effects were observed in the first two resonant regions. These results are not given in the present paper, however conclusions from them coincide with those for the three-mass system.

References

1. BOILER C., SEEGER T., 1987, *Materials Data for Cyclic Loading*, Parts A-E, Elsevier, New York
2. HAGEDORN P., 1981, *Non-Linear Oscillations*, Clarendon Press, Oxford

3. HALE J., 1977, *Theory of Functional Differential Equations*, Springer-Verlag, New York
4. MUSZYŃSKI J., MYSZKIS A.D., 1984, *Ordinary Differential Equations* [In Polish: *Równania różniczkowe zwyczajne*], PWN, Warszawa
5. NADOLSKI W., PIELORZ A., 1997, Nonlinear dynamic loads on gear teeth in discrete-continuous model of a single gear transmission, *Meccanica*, **32**, 165-168
6. PIELORZ A., 1988, Application of wave method in investigation of drive systems, comparison with other methods, *Mechanika Teoretyczna i Stosowana*, **26**, 97-112
7. PIELORZ A., 1999, Non-linear vibrations of a discrete-continuous torsional system with non-linearities having characteristic of a soft type, *Journal of Sound and Vibration*, **225**, 2, 375-389
8. PIELORZ A., SKÓRA M., 2006, Torsional vibrations of discrete-continuous systems with local nonlinearity having hard type characteristics, *Journal of Theoretical and Applied Mechanics*, **44**, 949-962
9. PONOMARIEV S.D. ET AL., 1957, *Modern Methods for Strength Calculations in Machine Design* [In Polish: *Współczesne metody obliczeń wytrzymałościowych w budowie maszyn*], T. I, PWN, Warszawa
10. STEWART H.B., THOMPSON J.M.T., UEDA Y., LANSBURY A.N., 1995, Optimal escape from potential wells – patterns of regular and chaotic bifurcation, *Physica D*, **85**, 259-295
11. SZEMPLIŃSKA-STUPNICKA W., 1990, *The Behavior of Nonlinear Vibrating Systems*, Vol. I, II, Kluwer Academic Publishers, Dordrecht
12. SZOLC T., 2003, *Dynamical Analysis of Complex Discrete-Continuous Mechanical Systems* [In Polish: *Analiza dynamiczna złożonych, dyskretno-ciągłych układów mechanicznych*], Habilitation Thesis, IFTR REPORTS, 2
13. THOMSON W.T., 1981, *Theory of Vibration with Applications*, Englewood Cliffs: Prentice-Hall

Drgania skrętne układów dyskretno-ciągłych z lokalną nieliniowością o charakterystyce typu miękkiego

Streszczenie

W pracy rozpatrywane są nieliniowe drgania wielomasowych układów mechanicznych odkształczanych skrętnie. Układy te złożone są z wałów połączonych dowolną liczbą brył sztywnych. W układach tych uwzględniono lokalną nieliniowość z charak-

terystyką typu miękkiego. Lokalna nieliniowość opisana jest za pomocą funkcji zawierających funkcje niewymierne oraz za pomocą dwóch innych funkcji nieliniowych. W rozważaniach wykorzystano podejście falowe. W analizie numerycznej skoncentrowano się na zbadaniu wpływu lokalnej nieliniowości na zachowanie się rozpatrywanych układów oraz na wyznaczeniu zakresów zastosowania funkcji niewymiernych. Przykładowe obliczenia numeryczne dotyczą układu trzymasowego.

Manuscript received February 27, 2008; accepted for print April 23, 2008